Scaling the Modulation Bandwidth and Phase Efficiency of a Silicon Optical Modulator

Ansheng Liu, Dean Samara-Rubio, Ling Liao, and Mario Paniccia

***Abstract*—We present an optimized design and detailed simulation of an all-silicon optical modulator based on a silicon waveguide phase shifter containing a metal-oxide-semiconductor (MOS) capacitor. Based on a fully vectorial Maxwell mode solver, we analyze the modal characteristics of the silicon waveguide. We show that shrinking the waveguide size and reducing gate oxide thickness significantly enhances the phase modulation efficiency because of the optical field enhancement in the voltage induced charge layers of the MOS capacitor, which, in turn, induce refractive index modulation in silicon due to free carrier dispersion effects. We also analyze the device speed by transient semiconductor device modeling. As both optical absorption and modulation bandwidth increase with increasing doping concentration, we show that, with a nonuniform doping profile in the waveguide, balance between the device operation speed and optical loss can be realized. Our simulation suggests that a TE-polarized optical phase modulator with a bandwidth of 10 GHz and an on-chip optical loss less than 2 dB is achievable in silicon.**

***Index Terms*—Metal-oxide-semiconductor (MOS) capacitor, optical modulator, phase shifter, planar lightwave circuits, silicon photonics, silicon-on-insulator (SOI), waveguide.**

I. Introduction

RECENT experimental demonstration of an all-silicon modulator with a modulation bandwidth exceeding 1 GHz [1] represents a significant enhancement in the speed of silicon based photonic devices as compared to conventional silicon modulators based on current injection in a forward-biased p-i-n diode in silicon [2]–[4]. This offers an opportunity for low-cost solutions to high-speed optoelectronic systems used in telecommunications, data communications, and chip-to-chip interconnect. The silicon modulator reported in [1] used a novel waveguide phase shifter containing a metal-oxide-semiconductor (MOS) capacitor. The applied voltage induced charge density change modifies the refractive index distribution in the waveguide. Although a bandwidth in excess of 1 GHz has been demonstrated in such a silicon modulator [1], one could anticipate even higher speed and better phase efficiency with appropriate device designs.

In this paper, we show that it is possible to achieve 10-GHz modulation frequency in a silicon MOS capacitor phase shifter. By use of a semiconductor device simulation tool, we model the transient response of the phase shifter. Modeling suggests that modulation speed is strongly dependent on the doping concentration and profile in the waveguide. Using a fully vectorial Maxwell waveguide mode solver, we simulate the phase modulation efficiency and optical loss of the phase shifter waveguide.

Manuscript received May 10, 2004; revised November 4, 2004.

The authors are with the Photonics Technology Laboratory, Intel Corporation, Santa Clara, CA 95054 USA (e-mail: ansheng.liu@intel.com).

Digital Object Identifier 10.1109/JSTQE.2005.845618

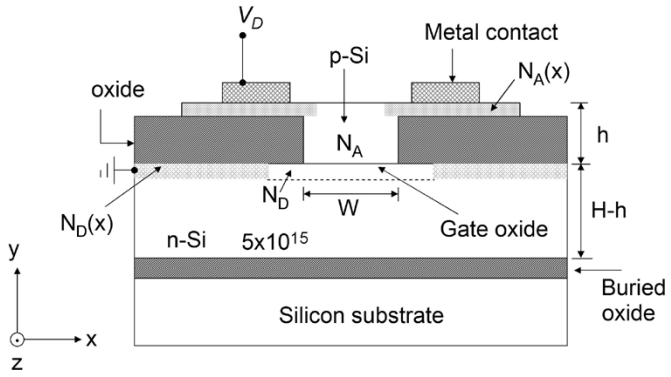

Fig. 1. Schematic diagram showing the cross-sectional view of a MOS capacitor waveguide phase shifter in silicon-on-insulator.

With a nonuniform doping profile, we show that an on-chip optical loss less than 2 dB is achievable for the 10-GHz modulator with a rib waveguide cross-section of approximately $1 \times 1\ \mu\mathrm{m}^2$.

Our paper is organized as follows. In Section II, we present design of the MOS capacitor based silicon waveguide phase shifter. We design a device with nonuniform doping profile in the waveguide to balance the device speed and optical loss. In Section III, we describe the theoretical background for the electrical and optical modeling. We show the voltage-induced charge density change in the MOS capacitor results in a phase modulation of the silicon waveguide phase shifter. We also outline the transient device simulation method. In Section IV, we first present detailed analysis of the influence of the gate oxide on the modal characteristics of the phase shifter and optimize the phase efficiency by waveguide scaling. We then analyze the device speed by electrical device simulation and show that high-speed (10 GHz) operation is achievable in a silicon modulator. We also present the optical loss modeling results for the optimized silicon phase shifter for 10-GHz operation. We present a conclusion in Section V.

II. Device Design

We consider a silicon MOS capacitor waveguide phase shifter. A cross-sectional view of such a structure is shown in Fig. 1. It comprises an n-type silicon slab (the silicon epitaxial layer of the SOI wafer) and a p-type single-crystal silicon rib with a gate oxide sandwiched between them. W, H and h denote the waveguide width, the total rib height, and the upper rib height, respectively (see Fig. 1). The gate oxide width is also W. We note that, in our previous experimental work [1], a p-type poly-silicon rib was used due to the device fabrication simplicity. Because poly-silicon exhibits higher optical loss as compared to single-crystal silicon [5], [6], an all-single-crystal

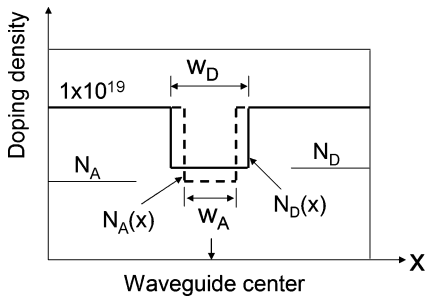

Fig. 2. Doping profiles $\mathrm{N_D(x)}$ and $\mathrm{N_A(x)}$ for the thin (0.15 μm) n-type and p-type silicon layers in the MOS capacitor phase shifter.

silicon modulator will have a lower optical transmission loss. However, we expect that the device speed would be quite similar between single-crystal silicon and partial poly-silicon modulators as long as the active doping concentration in poly-silicon is the same as that in single-crystal silicon. Also, we note that using the epitaxial lateral overgrowth technique [7], single-crystal silicon can be fabricated over the gate oxide.

To balance the optical loss of the phase shifter and the phase modulation speed, we consider a nonuniform doping profile in the waveguide. For both the n- and p-type regions, we divide each into two parts along the y direction. The lower part of the n-type silicon slab has a fixed low doping density of 5×10^{15} cm^{-3}. The upper part of the n-type silicon slab region has a shallow doping depth (the thickness is 0.15 μm) with a nonuniform doping concentration profile $\mathrm{N_D(x)}$ along the x direction. For the p-type silicon rib region, the doping concentration is assumed to be uniform with a doping density of $\mathrm{N_A}$ except for the thin top layer. The wide top p-type silicon layer has a thickness of 0.15 μm and also has a nonuniform doping concentration $\mathrm{N_A(x)}$ along the x axis. We assume that $\mathrm{N_D(x)}$ and $\mathrm{N_A(x)}$ have a piece-wise uniform profile along the x axis, as shown in Fig. 2. We note that in reality, the doping profile is not step-like. However, our electric and optical simulations show that the final results with a sharp and a smoother profile are only slightly different. Metal contacts are deposited on the shallow n- and p-type doped regions with a higher doping density of 1×10^{19} cm^{-3} and placed sufficiently away from the waveguide center to eliminate the optical absorption from the metal contacts. By varying the doping concentrations $\mathrm{N_A}$ and $\mathrm{N_D}$ near the waveguide center as well as the doping widths $\mathrm{W_A}$ and $\mathrm{W_D}$ defined in Fig. 2, one can change the device operation speed and the optical loss, as will be discussed in the following.

III. Electrical and Optical Modelling

When a positive voltage V_D is applied to the MOS capacitor phase shifter, a thin charge layer is accumulated on both sides of the gate oxide. The charge density changes ΔN_e (for electrons) and ΔN_h (for holes) are related to the drive voltage by [8]

$$\Delta N_e = \Delta N_h = \frac{\varepsilon_0 \varepsilon_r}{e t_{\mathrm{ox}} t}[V_D - V_{FB}] \tag{1}$$

where ε_0 and ε_r are the vacuum permittivity and low-frequency relative permittivity of the oxide, e is the electron charge, t_{ox} is the gate oxide thickness, t is the effective charge layer thickness, and V_{FB} is the flat band voltage of the MOS capacitor. For our devices, the device simulation suggests that the flat band voltage is $V_{FB} = 1.25$ V, and the effective charge layer thickness is $t = 10$ nm. This is consistent with the results in [1]. In the presence of free carriers, the optical properties of intrinsic silicon are modified due to the free carrier plasma dispersion effect [9], [10]. In the classical Drude model, the refractive index change (Δn) and optical absorption coefficient change $(\Delta\alpha)$ due to the free carriers in silicon are given by [9], [10]

$$\Delta n = -\frac{e^2\lambda^2}{8\pi^2 c^2 \varepsilon_0 n}\left[\frac{\Delta N_e}{m_e^*} + \frac{\Delta N_h}{m_h^*}\right] \tag{2}$$

$$\Delta\alpha = \frac{e^3\lambda^2}{4\pi^2 c^3 \varepsilon_0 n}\left[\frac{\Delta N_e}{m_e^{*2}\mu_e} + \frac{\Delta N_h}{m_h^{*2}\mu_h}\right] \tag{3}$$

where λ is the wavelength of light in free space, c is the velocity of light in vacuum, n is the refractive index of intrinsic silicon, m_e^* is the effective mass of electrons, m_h^* is the effective mass of holes, μ_e is the electron mobility, and μ_h is the hole mobility. Equations (2) and (3) indicate that both the refractive index and absorption coefficient changes have quadratic dependence on the wavelength. At the wavelength of interest (1.55 μm), the refractive index and absorption changes due to accumulated electrons and holes were obtained from experimental absorption spectra through Kramers–Kronig analysis by Soref and Bennett as [11]

$$\begin{aligned}\Delta n &= \Delta n_e + \Delta n_h \\ &= -8.8\times10^{-22}\Delta N_e - 8.5\times10^{-18}(\Delta N_h)^{-0.8}\end{aligned} \tag{4}$$

$$\begin{aligned}\Delta\alpha &= \Delta\alpha_e + \Delta\alpha_h \\ &= 8.5\times10^{-18}\Delta N_e + 6.0\times10^{-18}\Delta N_h\end{aligned} \tag{5}$$

where electron (ΔN_e) and hole (ΔN_h) density changes are in units of cm^{-3} and $\Delta\alpha$ is in units of cm^{-1}. The change in refractive index results in a phase shift $\Delta\phi$ in the optical mode given by

$$\Delta\phi = \frac{2\pi}{\lambda}\Delta n_{\mathrm{eff}} L \tag{6}$$

where L is the length of the phase shifter, Δn_{eff} is the change in the effective index of the fundamental waveguide mode before and after charge accumulation. To evaluate the phase shift, we employ a fully vectorial Maxwell waveguide solver based on the film mode matching method [12] to solve the waveguide mode. A complex effective index of the waveguide mode is obtained for a given waveguide dimension and doping distribution. The real part of the complex effective index is used to calculate the phase shift and the imaginary part is used to simulate the optical loss of the phase shifter.

As the phase modulation frequency is determined by the rate of the carrier density modulation in the device, one can model the transient response of the phase shifter to predict the device speed. To do so, we use a two-dimensional (2-D) device simulation package DESSIS. This device simulation tool employs the "box discretization" method [13] to solve the coupled Poisson equation and electron and hole continuity equations that govern charge transport in semiconductor devices. This is used to predict the electrical characteristics associated with specified physical structures and conditions. In addition, the simulation tool incorporates advanced semiconductor physics models to account for carrier statistics, doping and field dependent carrier mobility,

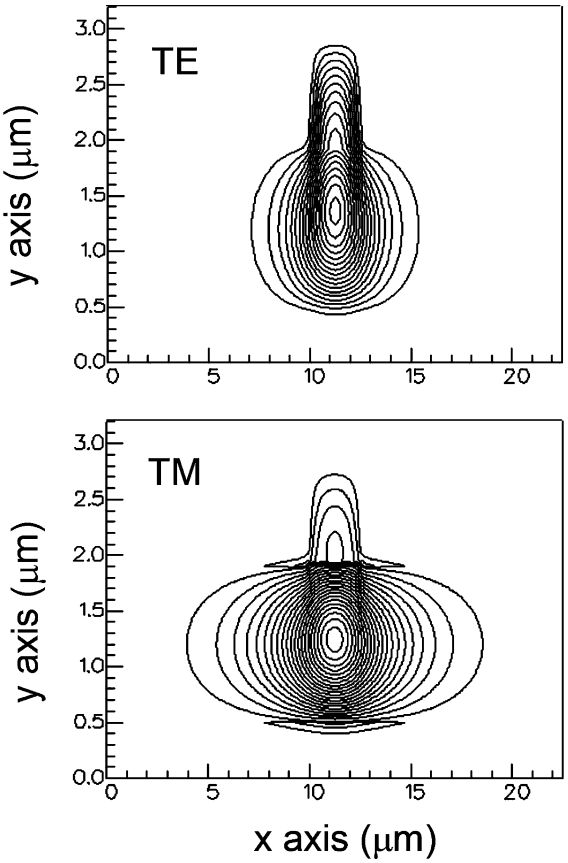

Fig. 3. Contour plot of modeled optical fields $|\mathrm{E_x}|$ for the TE mode and $|\mathrm{E_y}|$ for the TM mode for a waveguide phase shift of $\mathrm{W} = 2.5$, $\mathrm{H} = 2.3$, and $\mathrm{h} = 0.9$ μm. The gate oxide thickness is 120 Å. The wavelength is 1.55 μm.

and doping dependent carrier recombination lifetimes. In the transient device modeling, we apply a step-like drive voltage to the phase shifter and calculate the time dependence of the induced charge density at the oxide/silicon interfaces. The 3-dB modulation bandwidth Δf is then obtained from [14]

$$\Delta f = \frac{0.35}{T_r} \tag{7}$$

where T_r is the modeled rise time of the phase shifter in response to the step-like applied voltage (since the fall time is usually much shorter than the rise time because of the field induced carrier drift, the speed is primarily limited by the rise time). The rise time is defined as the duration during which the induced charge density in the MOS capacitor increases from 10 to 90% of its peak value.

IV. Results and Discussions

We first study the influence of the gate oxide on the modal characteristics of a silicon rib waveguide phase shifter. In the communication wavelength band (1.3–1.6 μm), the refractive index of gate oxide is much smaller than the index of silicon. Therefore, one would expect a notable change in the optical mode characteristics (effective index and mode profile) in the presence of a gate oxide in the silicon waveguide even when the gate oxide thickness is much smaller than the wavelength.

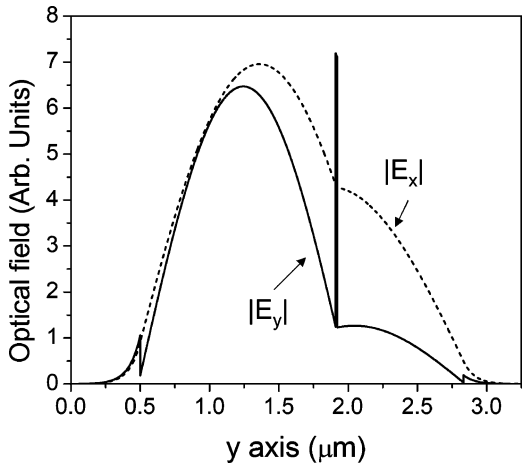

Fig. 4. Linecut of the modeled TE and TM mode profiles in Fig. 3 along the y direction at the waveguide center in the x direction.

Fig. 3 shows the modeled TE and TM mode profile at a wavelength of 1.55 μm for a waveguide with $\mathrm{W} = 2.5$, $\mathrm{H} = 2.3$, and $\mathrm{h} = 0.9$ μm. The gate oxide thickness is 120 Å. We see from Fig. 3 that there is a notable difference in the modeled TE and TM modes due to the presence of the gate oxide. The optical field for the TE polarized light is more tightly confined in the waveguide as compared to the TM polarized light. In particular, we note that the mode profile difference between the TE and TM modes is large in the vicinity of the gate oxide, as is evident from the linecut of the optical field along the y axis shown in Fig. 4. This is because the x component of the optical field (the major component for the TE mode) is continuous but the y component of the optical field (the major component for the TM mode) is discontinuous across the interfaces between silicon and oxide. Such a mode profile difference leads to a strong polarization dependent phase modulation of the MOS capacitor phase shifter, as the index modulation occurs only in the thin charge layer on both sides of the gate oxide. For the waveguide dimension in Fig. 3 with a drive voltage of $V_D = 6$ V, our modeling shows that $\mathrm{L}_\pi = 1.51$ cm for TE polarized light and $\mathrm{L}_\pi = 11.37$ cm for TM polarized light, where L_π is the phase shifter length required to produce a π phase shift and is a measure of the phase efficiency of the phase shifter for a given drive voltage. Note that the polarization dependent modulation efficiency is solely due to the modal difference of the waveguide phase shifter in the presence of the buried gate oxide, as the index change due to the free carrier dispersion effect is isotropic [see (2)]. Our modeling also shows that the TM mode is a leaky mode since the minor electrical field component (E_x) is not confined in the horizontal direction (confined in the vertical direction because of the high index contrast between silicon and oxide), although the major electric field component (E_y) is confined in both horizontal and vertical directions. Therefore, one would expect a higher waveguide loss for the TM polarized light compared to the TE polarized light, since both the major and minor components of the TE mode are confined. Since TE polarized light experiences higher phase modulation and lower optical loss as compared to TM polarized light, we will only consider TE polarized light in the rest of the paper.

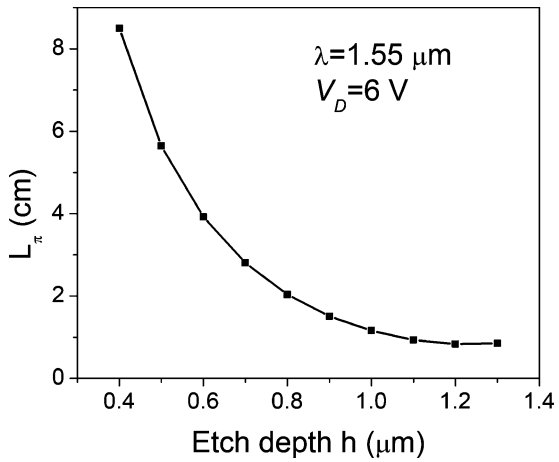

Fig. 5. Modeled L_π for a waveguide phase shifter as a function of the etch depth h. The waveguide width is $\mathrm{W} = 2.5\ \mu$m, the rib height is $\mathrm{H} = 2.3\ \mu$m. Gate oxide thickness is 120 Å. The wavelength is 1.55 μm, and the drive voltage is $V_D = 6$ V.

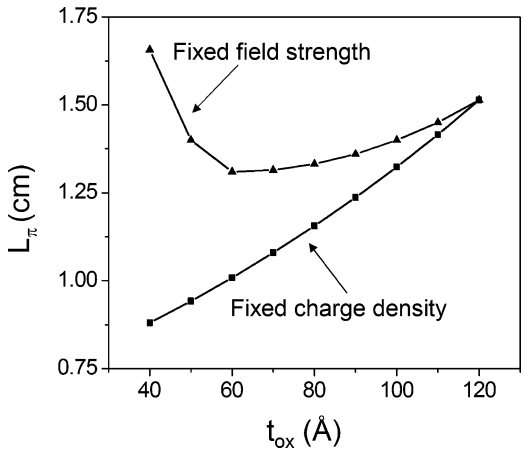

Fig. 6. Modeled L_π for a waveguide phase shifter as a function of the gate oxide thickness $\mathrm{t_{ox}}$. The waveguide width is $\mathrm{W} = 2.5\ \mu$m, the rib height is $\mathrm{H} = 2.3\ \mu$m, and etch depth is $\mathrm{h} = 0.9\ \mu$m. The wavelength is 1.55 μm. In the case of the fixed charge density, the drive voltage is varied while the gate oxide thickness is changed to keep the induced charge density constant equal to that for $t_{\mathrm{ox}} = 120$ Å and $V_D = 6$ V. For the fixed electrical field strength, we used 0.5 V/nm.

We now investigate the effect of the gate oxide position along the y direction on the phase modulation efficiency of our phase shifter. To this end, we model L_π for a waveguide with $\mathrm{W} = 2.5\ \mu$m and $\mathrm{H} = 2.3\ \mu$m at various etch depths. The result is shown in Fig. 5. In the modeling, we used a drive voltage of $V_D = 6$ V and a wavelength of 1.55 μm. We see from Fig. 5 that the phase efficiency is strongly dependent upon the gate oxide position. L_π decreases with increasing the etch depth. When the oxide is close to the center of the waveguide along the y direction (etch depth $\mathrm{h} = 1.2\ \mu$m), maximum phase efficiency (or minimum L_π) is obtained. There are two reasons that the phase efficiency increases with increasing the etch depth. First, the optical field in the charge layers increases when the gate oxide is closer to the waveguide center (see Fig. 4) so that the charge induced effective index change Δn_{eff} increases. Second, changing the etch depth also changes the lateral confinement of the rib waveguide. The larger the etch depth, the tighter the waveguide mode. Therefore, the larger confinement of the waveguide also contributes to the phase efficiency enhancement. In passing, we note that, when the etch depth is larger than 1.0 μm for the waveguide dimension of $\mathrm{W} = 2.5$ and $\mathrm{H} = 2.3\ \mu$m, the waveguide becomes a multimode device. In this case, the modeled L_π is for the fundamental mode. To keep the single mode operation, the phase efficiency of the device is not optimized when the waveguide dimension is large.

Since the optical mode is strongly influenced by the gate oxide, it is interesting to understand how the phase efficiency is dependent on the gate oxide thickness. Fig. 6 shows the modeled L_π for a waveguide with $\mathrm{W} = 2.5$, $\mathrm{H} = 2.3$, and $\mathrm{h} = 0.9\ \mu$m as a function of the gate oxide thicknesses at a wavelength of 1.55 μm. From (1) we note that, with a decrease in the gate oxide thickness, the applied voltage can be reduced proportionally to obtain the same charge density change. Reduction in the drive voltage not only simplifies the modulator driver circuitry design but also reduces the overall power dissipation. In order to study the sole effect of the gate oxide thickness on the phase efficiency due to the optical mode change, we can fix the voltage induced charge density change or the refractive index change while varying the gate oxide thickness. Thus, in the modeling of Fig. 6, we varied the drive voltage as the gate oxide thickness is changed to keep ΔN_e and ΔN_h fixed. We used $t_{\mathrm{ox}} = 120$ Å and $V_D = 6$ V as a reference and drive voltage was changed accordingly with the gate oxide thickness changes. For example, when $t_{\mathrm{ox}} = 60$ Å, the drive voltage is $V_D = 3.625$ V. We also note that the gate oxide breakdown voltage decreases with decreasing the gate oxide thickness. Therefore, for the thin gate oxide, the drive voltage cannot exceed the breakdown voltage (our experiment [1] shows that at the field strength of 1 V/nm the phase shifter is still functioning). In Fig. 6, we also show the modeled L_π as a function of the gate oxide thickness with a fixed electric field strength, i.e., $V_D/t_{\mathrm{ox}} = 0.5$ V/nm. We see from Fig. 6 that in the case of the fixed charge density, the phase efficiency monotonically increases with decreasing the gate oxide. This is because, when the gate oxide is thinner, the optical mode is less perturbed by the oxide layer so that the high optical field region of the guided mode overlaps more strongly with the regions of high charge density in the waveguide. In the case of the fixed electric field strength of 0.5 V/nm, the phase efficiency initially increases when the oxide thickness decreases. As expected, this phase efficiency increase is smaller than that for the case of the fixed charge density since for the fixed electric strength the voltage induced charge density decreases with decreasing the gate oxide thickness because of the flat band voltage [see (1)]. When t_{ox} is small (say < 60 Å), the phase efficiency decreases because the voltage induced charge density drops. There is an optimal gate oxide thickness giving the best phase efficiency.

To show the phase modulation efficiency of the phase shifter can be enhanced by the waveguide scaling, we model the phase shift as a function of the drive voltage for three different waveguide cross-section dimensions. The same gate oxide thickness of 120 Å is used for all the three devices. Simulation results of these devices are shown in Fig. 7. The devices are referred to in Fig. 7 as Devices A, B, and C, where Device A is the device reported in [1], which has waveguide dimensions of $\mathrm{W} = 2.5$, $\mathrm{H} = 2.3$, $\mathrm{h} = 0.9\ \mu$m. Device B is the device with waveguide dimensions of $\mathrm{W} = 1.5$, $\mathrm{H} = 1.5$, and $\mathrm{h} = 0.7\ \mu$m. Device C

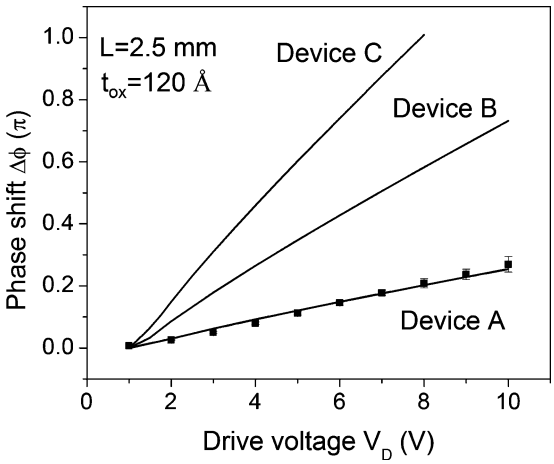

Fig. 7. Modeled phase shift $\Delta\phi$ of a 2.5-mm-long MOS capacitor phase shifter as a function of the drive voltage V_D at a wavelength of 1.55 μm for three different waveguide dimensions. Symbols represent the measured phase shift for Device A with p-type poly-silicon.

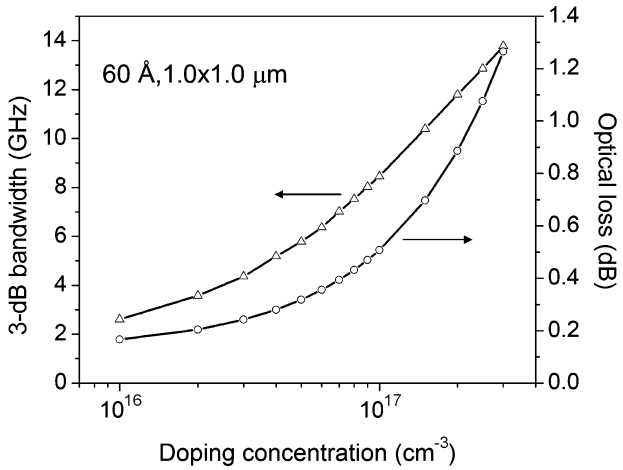

Fig. 8. Modeled 3-dB bandwidth and optical loss as a function of the doping concentration for Device C with a 60 Å gate oxide. The optical loss is for a device length that leads to $\pi/2$ phase shift at a drive voltage of $V_{\rm D} = 3$ V. The wavelength is $\lambda = 1.55$ μm.

is the device with waveguide dimensions of $\rm W = 1.0, H = 1.0$, and $\rm h = 0.5$ μm. Our modeling suggests that these waveguides are the single mode devices. Fig. 7 shows that reduction in waveguide dimensions significantly enhances the phase shift for a given device length ($\rm L = 2.5$ mm) and drive voltage. Such device scaling introduces design flexibilities enabling one to select convenient drive voltages and/or device lengths to be compatible with the chosen application. Fig. 7 also displays the experimentally measured phase shift for Device A with a p-type poly-silicon rib [1], which is in good agreement with simulations.

Now, let us discuss the device bandwidth. Since waveguide dimensions of Device C result in better phase modulation efficiency, we used this device to model the bandwidth as a function of the doping concentration. A gate oxide thickness of 60 Å is chosen because it leads to higher phase efficiency as shown in Fig. 6. In addition, a thinner gate gives rise to higher capacitance of the MOS capacitor. Thus, speed modeling of a device with thinner gate oxide predicts a lower speed limit, because for the same doping concentration, the RC time constant is smaller for smaller capacitance. In the simulation, we assumed that $\rm N_A = N_D$ and the doping widths are $\rm W_A = 1.0$ and $\rm W_D = 2.0$ μm (see Fig. 2 for the doping profile). The simulated results are shown in Fig. 8. We see from Fig. 8 that the 3-dB modulation bandwidth increases with an increase in the doping concentration. When the doping level reaches $\sim 1.5 \times 10^{17}$ cm^{-3}, a 10-GHz bandwidth is obtained. Fig. 8 also shows that the modulation bandwidth can be scaled to even higher values with higher doping concentrations. In passing, we note that the modeled speed of the silicon modulator in [1] is 2.03 GHz by using the measured electrically activated doping concentrations. The measured modulation bandwidth is ~2.5 GHz [1], which is slightly higher than the modeled value. We also note that the actual device operation speed depends on not only the intrinsic bandwidth of the phase shifter but also the drive circuitry. As the device speed was modeled by a two-dimensional (2-D) semiconductor simulator, the electrode length effect on the speed was not considered. For high bandwidth (>10 GHz) and for a longer phase shifter, travelling-wave electrodes [15] may be needed.

It is also worth noting that increasing the modulation speed by increasing doping concentrations also increases the static loss (the "off state" optical loss) due to free carrier absorption, as is evident from (3). To quantify such effects, we modeled the phase shifter loss as a function of the doping concentration for Device C. As the phase shifter length is only required to achieve $\pi/2$ phase shift for the push-pull operation [16] in a Mach–Zehnder interferometer (MZI) modulator, we calculated the phase shifter loss for a device length of $L_{\pi/2}$. For Device C, with a gate oxide of 60 Å and at $V_{\rm D} = 3$ V, the modeled $L_{\pi/2} = 1.94$ mm. Fig. 8 shows that the optical loss of the phase shifter increases with increasing the doping concentration. For a concentration of $\sim 1.5 \times 10^{17}$ cm^{-3}, which leads to 10-GHz modulation bandwidth, the modeled phase shifter loss is ~0.7 dB. We note here that ~0.7 dB is the passive phase shifter loss without applied voltage. Additional loss (~1 dB) for required $\pi/2$ phase shift due to voltage induced free carrier absorption should be included in the MZI loss in the "on" state, in which the optical transmission of the modulator reaches the maximum value. In addition, the MZI modulator loss will also include the Y junction loss and passive waveguide loss due to light scattering-induced, for example, by sidewall roughness. With development of the advanced fabrication technology, it is expected that these losses could be minimal, as low transmission loss in small waveguides on SOI is well established [17], [18]. To realize efficient light coupling between optical fiber and small silicon waveguide, a mode-size converter is usually required. Development of such a low loss taper in SOI is challenging but some progress has been made [19], [20].

V. Conclusion

Based on semiconductor device and optical mode simulations, we have analyzed the phase modulation efficiency of a MOS capacitor based silicon waveguide phase shifter. It was demonstrated that scaling down the waveguide dimension significantly enhances the phase efficiency. We also investigated the intrinsic modulation speed of the phase shifter. We have shown that high-speed operation of the silicon phase shifter with

a bandwidth of 10 GHz is achievable with appropriate choices of the doping density and profile. The associated optical phase shifter loss was also modeled. Simulation shows that a silicon modulator with bandwidth of 10 GHz and an on-chip loss less than 2 dB could be fabricated.

ACKNOWLEDGMENT

The authors would like to thank M. Morse, M. Salib, D. Rubin, and O. Cohen for discussions on possible process implementation, and Prof. G. T. Reed of the University of Surrey for useful discussions.

REFERENCES

[1] A. Liu, R. Jones, L. Liao, D. Samara-Rubio, D. Rubin, O. Cohen, R. Nicolaescu, and M. Paniccia, "A high-speed silicon optical phase modulator based on a metal-oxide-semiconductor capacitor," *Nature*, vol. 427, pp. 615–618, Feb. 2004.

[2] G. V. Treyz, P. G. May, and J. M. Halbout, "Silicon Mach-Zehnder waveguide interferometers based on the plasma dispersion effect," *Appl. Phys. Lett.*, vol. 59, pp. 771–773, Aug. 1991.

[3] C. K. Tang and G. T. Ree, "Highly efficient optical phase modulator in SOI waveguides," *Electron. Lett.*, vol. 31, pp. 451–452, Mar. 1995.

[4] P. Dainesi, A. Kung, M. Chabloz, A. Lagos, P. Fluckiger, A. Ionescu, P. Fazan, M. Declerq, P. Renaud, and P. Robert, "CMOS compatible fully integrated Mach-Zehnder interferometer in SOI technology," *IEEE Photon. Technol. Lett.*, vol. 12, no. 6, pp. 660–662, Jun. 2000.

[5] L. Liao *et al.*, "Optical transmission losses in polycrystalline silicon strip waveguides: Effects of waveguide dimensions, thermal treatment, hydrogen passivation, and wavelength," *J. Electron. Mater.*, vol. 29, pp. 1380–1386, 2000.

[6] L. Liao, "Low loss polysilicon waveguides for silicon photonics," M.S. thesis, Massachusetts Institute of Technology, Cambridge, MA, 1997.

[7] S. S. Ahmed, J. P. Denton, and G. W. Neudeck, "Nitride thermal SiO_2 for use as top and bottom gate insulators in self-aligned double gate silicon-on-insulator metal-oxide-semiconductor field effect transistor," *J. Vac. Sci. Technol. B*, vol. 19, pp. 800–806, 2001.

[8] S. M. Sze, *Physics of Semiconductor Devices*, 2nd ed. New York: Wiley, 1981.

[9] R. A. Soref and P. J. Lorenzo, "All silicon active and passive guided-wave components for $\lambda = 1.3$ μm and 1.6 μm," *IEEE J. Quantum Electron.*, vol. QE-22, no. 6, pp. 873–879, Jun. 1986.

[10] R. A. Soref and B. R. Bennett, "Electrooptical effects in silicon," *IEEE J. Quantum Electron.*, vol. QE-23, no. 1, pp. 123–129, Jan. 1987.

[11] ——, "Kramers-Kronig analysis of electro-optical switching in silicon," in *Proc. SPIE*, vol. 704, Sep. 1986, pp. 32–37.

[12] A. S. Sudbo, "Numerically stable formulation of the transverse resonance method for vector mode-field calculations in dielectric waveguides," *IEEE Photon. Technol. Lett.*, vol. 5, no. 3, pp. 342–344, Mar. 1993.

[13] R. E. Bank, W. M. Coughran, Jr.., W. Fichtner, E. H. Grosse, D. J. Rose, and R. K. Smith, "Transient simulation of silicon devices and circuits," *IEEE Trans. Computer-Aided Design*, vol. CAD-4, no. 4, pp. 436–451, Oct. 1985.

[14] G. P. Agrawal, *Fiber-Optic Communication Systems*, 2nd ed. New York: Wiley, 1997.

[15] K. S. Giboney, M. J. W. Rodwell, and J. E. Bowers, "Travelling-wave photodetector design and measurements," *IEEE J. Sel. Topics Quantum Electron.*, vol. 2, no. 3, pp. 622–628, Sep. 1996.

[16] J. C. Cartledge, "Performance of 10 Gb/s lightwave systems based on lithium niobate Mach-Zehnder modulators with asymmetric Y-branch waveguides," *IEEE Photon. Technol. Lett.*, vol. 7, no. 9, pp. 1090–1092, Sep. 1995.

[17] K. K. Lee, D. R. Lim, L. C. Kimerling, J. Shin, and F. Cerrina, "Fabrication of ultralow-loss Si/SiO_2 waveguides by roughness reduction," *Opt. Lett.*, vol. 26, pp. 1888–1890, Dec. 2001.

[18] S. Lardenois, D. Pascal, L. Vivien, E. Cassan, S. Laval, R. Orobtchouk, M. Heitzmann, N. Bouzaida, and L. Mollard, "Low-loss submicrometer silicon-on-insulator rib waveguides and corner mirrors," *Opt. Lett.*, vol. 28, pp. 1150–1152, Jul. 2003.

[19] T. Shoji, T. Tsuchizawa, T. Watanabe, K. Yamada, and H. Morita, "Low loss mode size converter from 0.3 μm square Si wire waveguides to singlemode fibers," *Electron. Lett.*, vol. 38, pp. 1669–1679, Dec. 2002.

[20] G. Z. Masanovic, V. M. N. Passaro, and G. T. Reed, "Dual grating-assisted directional coupling between fibers and semiconductor waveguides," *IEEE Photon. Technol. Lett.*, vol. 15, no. 10, pp. 1395–1397, Oct. 2003.

Ansheng Liu received the Ph.D. degree from the University of Aalborg, Aalborg, Denmark, in 1992.

He is currently a Research Scientist and Senior Staff Member with the Photonics Technology Laboratory, Intel Corporation, Santa Clara, CA, where he is developing silicon photonic devices in the Corporate Technology Group. Before joining Intel in 2000, he worked at NASA Ames Research Center, the National Institute of Standards and Technology, and at the University of Aalborg as an Assistant Professor. His research interests include nonlinear optics of nanostructures, near-field optics, optoelectronics, and photonics.

Dean Samara-Rubio received the B.S. degree in electrical engineering from the University of Illinois, Urbana-Champaign, in 1991, and the Ph.D. degree in electrical engineering from the University of Texas, Austin, in 1997.

He is currently a Senior Researcher with the Photonics Technology Laboratory, Intel Corporation, Santa Clara, CA. His research interests include the design of integrated circuits and optical components, optoelectronic characterization, and silicon modulator project management.

Ling Liao received the B.S. and M.S. degrees in materials science and engineering from the Massachusetts Institute of Technology, Cambridge.

She is a currently a Senior Researcher with the Photonics Technology Laboratory, Intel Corporation, Santa Clara, CA. Her research interests include silicon photonics and high-speed optical modulation.

Mario Paniccia received the B.S. degree in physics from the State University of New York, Binghamton, and the Ph.D. degree in solid state physics from Purdue University, West Lafayette, IN.

He is currently Director of the Photonics Technology Laboratory, Intel Corporation, Santa Clara, CA, where he leads a research team focused on developing silicon-based photonic building blocks using standard CMOS processing for future use in enterprise and data center communications.